Research Article

Received: 4 December 2020 Revised: 22 January 2021 Accepted article published: 27 January 2021 Published online in Wiley Online Library:

(wileyonlinelibrary.com) DOI 10.1002/jctb.6685

Deactivation and regeneration of Pt-modified zeolite Beta–Bindzil extrudates in *n*-hexane hydroisomerization

Zuzana Vajglová,[a] Narendra Kumar,[a] Markus Peurla,[b] Leena Hupa,[a] Kirill Semikin,[c] Dmitry A Sladkovskiy[c] and Dmitry Yu Murzin[a]*

Abstract

BACKGROUND: The metal–acid bifunctional catalysts are widely used in many industrially significant chemical processes, including hydroisomerization of *n*-hexane. Deactivation and regeneration of metal–acid bifunctional extrudates was investigated in continuous *n*-hexane hydroisomerization in a fixed-bed reactor. Four Pt/H-Beta-25 catalysts containing 30% Bindzil binder were prepared with the same composition and controlled metal deposition.

RESULTS: Different preparation steps led to differences in the mechanical strength, Pt particle size, acidity and strength, metal-to-acid site (c_{Pt}/c_{AS}) ratio and proximity between two types of active sites. A very slow deactivation and high selectivity to C_6 isomers was obtained when Pt was deposited on H-Beta-25 zeolite.

CONCLUSION: Initial selectivity to the desired products was correlated with the physicochemical properties of the catalysts. Location of the metal has a larger influence on catalyst deactivation of the bifunctional catalysts rather than the metal-to-acid site ratio or site proximity. Decline of *n*-hexane conversion and selectivity to C_6 isomers were correlated with changes in the textural properties and acidity of the deactivated catalyst, respectively.

Keywords: *n*-hexane hydroisomerization; shaped catalyst; metal location; deactivation

INTRODUCTION

Metal–acid bifunctional catalysts are widely used in many industrially significant chemical processes, e.g. hydrocracking of heavy oils, dewaxing, reforming, selective ring opening and hydroisomerization.[1–9] Hydroisomerization of C_5–C_6 *n*-alkanes involving three steps, namely dehydrogenation of alkanes, skeletal isomerization of olefins and hydrogenation of the latter, is one of the cheapest ways to improve fuel quality (increase in octane number).[3,4,9–11] The de/hydrogenation steps occur on the metallic sites (e.g. Pt, Pd, Mo, W, Co, Ni), while isomerization or hydrocracking steps proceed on the acid sites (e.g. amorphous silica–alumina oxides, zeolites and mesoporous aluminosilicates).[1–3,5,9,12]

Diffusion of the olefinic intermediates between metallic and acidic sites is very important and therefore design of the metal–acid bifunctional catalysts plays a key role in the hydroisomerization of straight-chain paraffins. The controlled acidity (Brønsted and Lewis) in terms of strength and the number of the acid sites, metal–acid balance and proximity between these two types of active sites should mainly be taken into account for optimal performance of bifunctional catalytic systems.[2–5,8–10,12–17]

Many studies of metal–acid bifunctional catalysts have been performed with powder catalysts under the kinetic regime.[1,11,16,18–28] However, in an industry where shaped catalytic bodies containing binders are used, the mass transport limitation regime is almost unavoidable. Not only mass transfer limitations but also changes in physicochemical properties of a catalyst due to its scale-up process can lead to a significantly different product distribution as well as catalyst deactivation compared to fine catalyst powders. During the scale-up of zeolite-based catalysts by extrusion, organic and inorganic binders are typically added to improve plasticity of the extruded paste and to improve the mechanical resistance of shaped zeolites, respectively. Chemical interactions between the catalyst and the binder, and the shaping process per se, can have a significant effect on the physicochemical properties of the final extrudates.[2,3,22,29–39]

* *Correspondence to: DY Murzin, Åbo Akademi University, Johan Gadolin Process Chemistry Centre, Biskopsgatan 8, Turku/Åbo 20500, Finland. E-mail: dmurzin@abo.fi*

a *Åbo Akademi University, Johan Gadolin Process Chemistry Centre, Turku/Åbo, Finland*

b *Institute of Biomedicine, University of Turku, Turku, Finland*

c *Resource Saving Technologies Department, St Petersburg State Institute of Technology, St Petersburg, Russia*

Several studies on C_7–C_{16} *n*-alkane hydroisomerization used crushed shaped Pt catalysts (0.1–0.8 mm) with Pt deposition on either the shaped supports[1,2,40,41] or on a zeolite.[1,2,21,42] However, detailed studies of the uncrushed shaped bifunctional catalysts are still lacking in the open literature.[2,3] Our recent work on *n*-hexane hydroisomerization over Pt/H-Beta-25 extrudates containing bentonite binder[3] revealed that at low temperature the performance of a bifunctional shaped catalyst was strongly affected by the metal-to-acid site ratio (c_{Pt}/c_{AS}). The highest conversion of *n*-hexane and selectivity to C_6 isomers was obtained over extrudates with the highest c_{Pt}/c_{AS} ratio and their closest proximity; i.e. when Pt was located exclusively on the zeolite.

The current work continues our recent efforts[3] to improve fundamental knowledge on the scaling up of metal–acid bifunctional catalysts for straight-chain paraffin hydroisomerization. This study is focused on the effect of the preparation of Pt/H-Beta-25 bifunctional extrudates with controlled metal deposition on the catalyst deactivation and regeneration in continuous *n*-hexane hydroisomerization in a fixed-bed reactor. In order to avoid the effect of impurities (Fe_2O_3, K_2O, MgO) in the bentonite binder,[31] colloidal silica (Bindzil-50/80) was used as an inorganic binder.

EXPERIMENTAL

Preparation of the shaped Pt catalysts

For the preparation of four Pt/H-Beta-25 extrudates with the controlled metal deposition (Fig. 1), the same procedure as in our previous work[3] was used. The main difference was in using, as a binder, colloidal silica Bindzil-50/80 (50 wt% SiO_2 in water, Akzo Nobel) instead of bentonite applied previously. The composition was the same for all catalysts, i.e. 2 wt% of Pt nominal loading and 70/30 weight ratio of H-Beta-25 zeolite/Bindzil binder. Tetraammonium-platinum(II) nitrate (≥50% Pt basis, Sigma-Aldrich) was used as a source of Pt precursor. In the case of catalyst A, the composite material was first synthesized, then shaped into a cylindrical body of 1.5 mm in diameter by extrusion in a one-screw extruder (TBL-2, Tianjin Tianda Beiyang Chemical Co. Ltd) from the slurry containing 1% methylcellulose, and, finally, Pt was introduced by the evaporation impregnation method. In the case of catalyst B, Pt was introduced into the zeolite–binder composite material, and then shaped. For catalysts C and D, Pt was introduced either on the Bindzil binder or H-Beta-25, respectively, then synthesized with the corresponding counterpart (i.e. the zeolite or the binder, respectively), and finally shaped. The proton form of Beta-25 zeolite was obtained from commercial NH_4-Beta-25 (SiO_2/Al_2O_3 = 25, CP814E, Zeolyst International) by calcination in a muffle oven at 500 °C for 4 h.

Physicochemical characterization of shaped Pt catalysts

The four fresh and spent extrudates were characterized by several methods. Transmission electron microscopy (TEM) (JEOL JEM-1400Plus) was used to measure the metal (Pt) particle size and determine whether the metal was deposited on H-Beta-25 or on the Bindzil binder. The surface morphology, interphase interactions and Pt concentration on the outer layer of extrudates were studied by scanning electron microscopy–energy-dispersive X-ray analysis (SEM-EDX; Zeiss Leo Gemini 1530). The Pt concentration in the entire volume of the shaped catalyst body was determined by inductively coupled plasma–optical emission spectroscopy (ICP-OES; PerkinElmer Optima 5300 DV). The mechanical strength of extrudates was measured using a crush test (SE 048, Lorentzen & Wettre). Fourier transform infrared (FTIR; ATI Mattson FTIR Infinity Series spectrometer) was used to determine the strength and quantification of Brønsted and Lewis acidity with pyridine desorption at 250–350, 350–450 and 450 °C, reflecting weak, medium and strong acid sites. Textural properties were measured by nitrogen physisorption (Micromeritics 3Flex-3500). Details of the physicochemical characterization methods and equipment are presented in our previous publications.[3,29–32]

Catalytic tests of *n*-hexane hydroisomerization in the fixed-bed reactor

Experiments in the continuous mode were performed with Pt/H-Beta-25 cylindrical extrudates containing 30 wt% Bindzil binder (diameter 1.5 mm, length 3.0 mm). Hydroisomerization of *n*-hexane (Fig. 2) was selected as a model reaction. The reaction was performed over 3 g Pt extrudates in a fixed-bed reactor (12 mm in diameter, catalyst zone of 70 mm, thermocouple pocket of 3 mm, reactants flow from top to bottom, a turbulizer upstream of the catalytic zone).[3] Before the reaction, the catalyst was flushed with nitrogen and then reduced under a hydrogen flow rate of 30 mL min^{-1} at 400 °C and 1 bar for 1 h. The catalytic tests were divided into two stages: the first stage was focused on measuring stable catalyst activity and in the second stage the catalyst was measured under deactivation conditions. The reaction conditions were: 250 °C, 1 bar H_2, constant 50 mL min^{-1} He flow rate through the vessel containing liquid *n*-hexane, and 30 and 5 mL min^{-1} H_2 flow rate for the first and second stage, respectively. After the reaction, the spent catalyst was regenerated via the following procedure: the spent catalyst was calcined at 600 °C for 3 h (heating rate 350 °C h^{-1}), flushed with nitrogen, reduced according to the same program as mentioned above and reused.

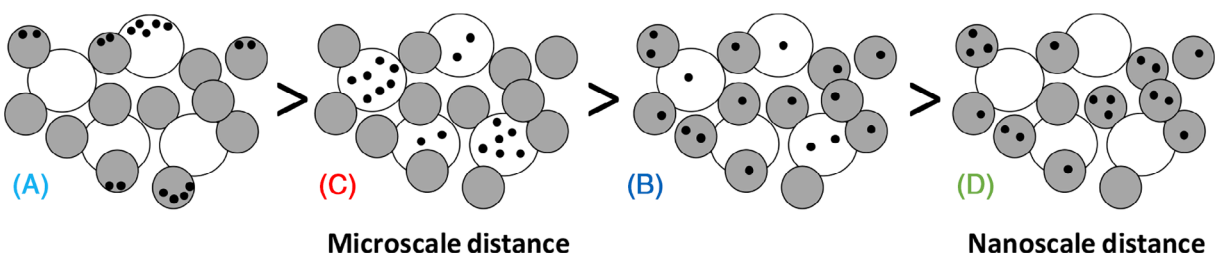

Figure 1. Schematic picture of the catalysts employed in this study, showing different Pt location and distances between the metal and acid sites. A: Pt/(H-Beta-25 + Bindizl-50/80), post synthesis; C: (Pt/Bindizl-50/80) + H-Beta-25, *in situ* synthesis; B: Pt/(H-Beta-25 + Bindizl-50/80), *in situ* synthesis; D: (Pt/H-Beta-25) + Bindizl-50/80, *in situ* synthesis. H-Beta-25 (grey circle), Bindizl-50/80 (white circle), Pt (black dots).[1,3]

Journal of Chemical Technology & Biotechnology published by John Wiley & Sons Ltd on behalf of Society of Chemical Industry.

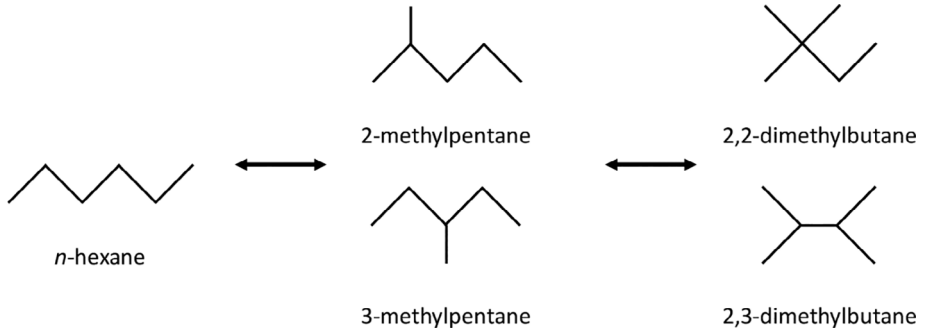

Figure 2. Hydroisomerization of *n*-hexane.[3]

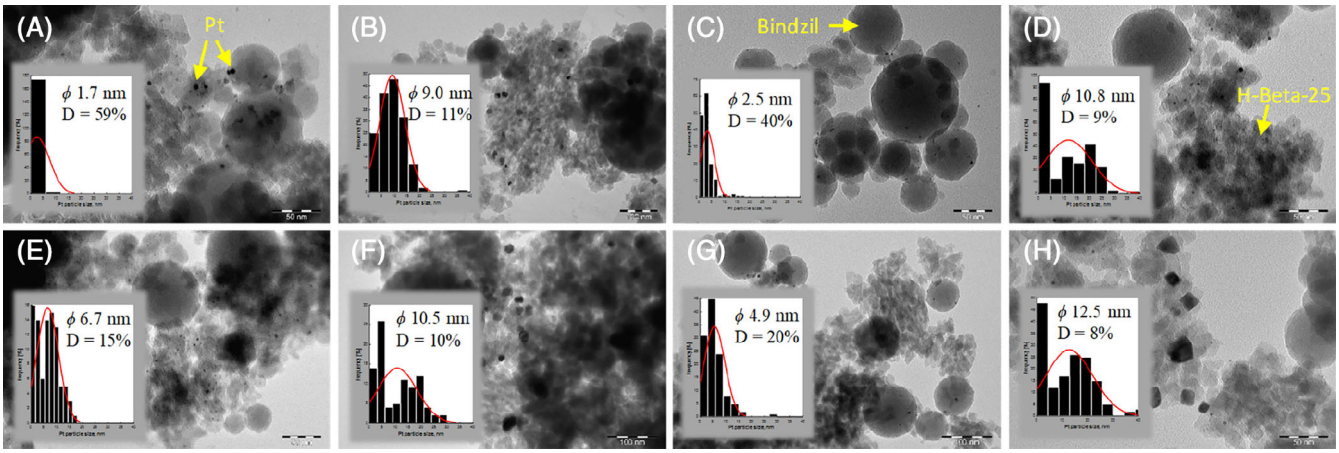

Figure 3. TEM images: (a, e) fresh and spent Pt/(H-Beta-25 + Bindzil), post synthesis; (b, f) fresh and spent Pt/(H-Beta-25 + Bindzil), *in situ* synthesis; (c, g) fresh and spent (Pt/Bindzil) + H-Beta-25; (d, h) fresh and spent (Pt/H-Beta-25) + Bindzil. D, metal dispersion ($100/d_{Pt}$).

RESULTS AND DISCUSSION

Physicochemical characterization results of shaped Pt catalyst

In line with our previous studies,[3,29] TEM images (Fig. 3) confirmed the applicability of the proposed approach to prepare materials with controlled metal (Pt) deposition. Small Pt particle sizes were obtained for catalyst A prepared via the post-synthesis method with a random metal location on both H-Beta-25 zeolite and Bindzil binder (ϕ 1.7 nm, min 0.2, max 26 nm) and for catalyst C, where the metal was located exclusively on Bindzil (ϕ 2.5 nm, min 0.5, max 17 nm). Approximately fivefold larger Pt particle sizes were measured for catalyst B prepared via *in situ* synthesis method with a random metal (Pt) location (ϕ 9.0 nm, min 1.1, max 39 nm) and for catalyst D, where the metal was deposited exclusively on H-Beta-25 (ϕ 10.8 nm, min 0.9, max 44 nm). The size of Pt clusters in the case of catalyst A, which was relatively smaller than for other materials, can be related to the impregnation procedure. In the former case Pt was introduced from an aqueous solution of $Pt(NH_3)_4(NO_3)_2$ onto a shaped catalyst, followed by its slow penetration from the outer layer into the interior of the extrudate. In other cases, i.e. for catalysts B, C and D, platinum was introduced into the powder material, followed by shaping. After the reaction, the Pt particle sizes slightly increased, on average, giving also a broader distribution with a shift to larger Pt particle sizes. Significant sintering of metal particles (Fig. 3) was observed for catalysts A and C with the microscale distance between metal and acid sites (Fig. 1). This could be related to local overheating by the exothermic reaction on the spots with high size density, leading to the diffusion of metal particles and subsequent to meeting each other. Another explanation may be the lower binding of metal support in the case of silica binder compared to zeolite.

SEM images (Fig. 4) showed the local interphase interactions caused by the agglomeration step in the catalyst–binder preparation[30] and by extrusion.[3,29,31,32] The observed significant intracrystalline void space between the particles in the catalyst C could be a reason for lower mechanical strength (2.9 and 0.7 MPa in the vertical and horizontal position, respectively; Table 1). The mechanical strength for other Pt/H-Beta-25 extrudates containing 30 wt% Bindzil (3.8–4.5 MPa in the vertical position, Table 1) was higher and comparable with Pt/H-Beta-25 extrudates containing 30 wt% bentonite binder (3.2–4.8 MPa).[3] Hence chemical interactions between the catalytically active phases of Pt/H-Beta-25 and the Bindzil binder are important for enhancing the mechanical strength of the synthesized extrudates. Furthermore, enhancement of such interactions between the active phases and the binder is influenced by selection of organic and inorganic binders, the particle size of the catalytic active phase, as well as rheological properties of the paste for extrusion. Methods of metal introduction, synthesis temperature, time and activation procedures are important parameters, which should be taken into consideration for preparation of mechanically stable extrudates with an enhanced strength.

Real Pt concentration, determined by ICP-OES in the entire volume of the shaped body, was the same as the nominal loading (2 wt%) for catalysts A and B, where Pt was deposited randomly

Journal of Chemical Technology & Biotechnology published by John Wiley & Sons Ltd on behalf of Society of Chemical Industry.

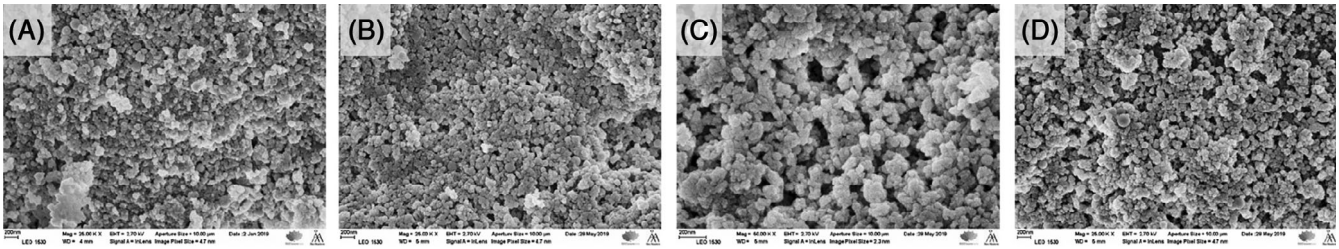

Figure 4. SEM images: (a) Pt/(H-Beta-25 + Bindzil), post synthesis; (b) Pt/(H-Beta-25 + Bindzil), *in situ* synthesis; (c) (Pt/Bindzil) + H-Beta-25; (d) (Pt/H-Beta-25) + Bindzil.

Table 1. Characterization results of shaped Pt catalysts with controlled metal location

	MS_v (MPa)	MS_h (MPa)	c_{Pt} (%)	c_{Pt_E} (%)	BAS (μmol g^{-1})				LAS (μmol g^{-1})				TAS (μmol g^{-1})	c_{Pt}/c_{AS}
					w	m	s	Σ	w	m	s	Σ		
E[31]	3.5	1.3	—	—	50	17	77	145	25	2	2	30	175	—
A–F	4.5	1.8	2.0	3.5	61	1	0	62	26	0	0	26	88	0.68
B–F	4.4	1.2	2.0	1.7	62	2	3	67	0	1	0	1	68	0.16
C–F	2.9	0.7	1.7	1.0	49	5	7	61	1	1	0	2	63	0.54
D–F	3.8	1.2	2.3	1.2	42	0	1	43	3	0	0	3	46	0.24
A–S	—	—	—	—	129	14	0	142	6	1	0	8	150	—
B–S	—	—	—	—	833	6	0	840	14	2	0	15	855	—
C–S	—	—	—	—	52	18	0	71	3	2	0	5	75	—
D–S	—	—	—	—	60	2	0	62	4	0	0	4	66	—

E: data from literature[31] for metal-free H-Beta-25 extrudates containing 30% of the Bindzil binder: F: fresh catalyst: S: spent catalyst; A: Pt/(H-Beta-25 + Bindzil), post synthesis; B: Pt/(H-Beta-25 + Bindzil), *in situ* synthesis; C: (Pt/Bindzil) + H-Beta-25; D: (Pt/H-Beta-25) + Bindzil; BAS: Brønsted acid sites; LAS: Lewis acid sites; TAS: total acid sites; w: weak; m: medium; s: strong; c_{Pt_E}: Pt concentration at the top of the extrudate surface; c_{Pt}: Pt concentration in the entire volume; c_{AS}: concentration of total acid sites; MS: mechanical strength of extrudates in vertical (v) and horizontal (h) position.

on both H-Beta-25 and Bindzil. A slightly higher (2.3 wt%) and, conversely, a lower (1.7 wt%) Pt concentration was obtained for catalysts D and C, respectively. Pt concentration on the outer layer of extrudates determined by EDX revealed the higher value (3.5 wt%) for the catalyst A prepared via the post-synthesis method, as expected. However, this value was ~2.4 lower compared to the eggshell type of Pt/H-Beta-25 extrudates containing bentonite.[3] These results could be attributed to better penetration of Pt into the extrudates for the Bindzil binder (i.e. colloidal silica without impurities) than for bentonite.

The highest (88 μmol g^{-1}) and the lowest total acid sites (46 μmol g^{-1}, i.e. about twofold lower than the highest value) were obtained for catalysts A and B, respectively (Table 1). For catalysts B and D, the total acid sites (68 and 63 μmol g^{-1}, respectively) were comparable. The same trend was observed for Pt extrudates with bentonite, even though the total acid sites were about twofold higher (69–208 μmol g^{-1}).[3] It is noteworthy that a significantly higher Lewis acidity was detected for catalyst A as compared other materials (Table 1). After the catalytic tests, total acidity was increased in all cases, mainly due to increasing weak and medium Brønsted acid sites (Table 1). A significant increase of acidity (~12.6-fold) accompanied by a shift in the peak for Brønsted acid sites (from 1550 to 1650 s^{-1}) was observed for catalyst B. This could be attributed to coke formation during deactivation.

Differences in the number of total acid sites between catalysts with the same composition and the same nominal loading of Pt can be attributed to different synthesis procedures, in particular the step where the metal precursor was introduced onto supports of different acidity. In line with the work of Kubička *et al.*,[43] deposition of platinum on zeolites led to changes in acidity compared to the pristine supports. This subsequently affected the acidity of the final extrudates and thus the metal-to-acid site (c_{Pt}/c_{AS}) ratio. For Pt extrudates with Bindzil, different metal-to-acid site ratios (c_{Pt}/c_{AS} = 0.16–0.68, Table 1) in a narrower range were obtained compared to Pt extrudates with bentonite as a binder (0.07–1.12).[3] This can be attributed to significantly different ranges of catalyst acidity, as mentioned above. The work of Kubička *et al.*[43] states that also the electronic properties of Pt are influenced by acidic supports, with the magnitude of such alterations being dependent on the support acidity.

In line with the literature,[3,29,31,32] the textural properties were similar, but the specific surface area was slightly lower for catalyst B (Fig. 5). After the reaction, the surface area decreased by ~10% for catalysts A, C and D. A significantly higher decrease in the surface area and the pore volume by 44% and 27%, respectively, was observed for catalyst B (Fig. 5). This could be related to coking of the catalyst surface, as mentioned above as an explanation for increased acidity.

Catalytic activity, selectivity and stability of shaped Pt-catalysts in *n*-hexane hydroisomerization

Fresh and regenerated Pt extrudates with Bindzil were tested in two stages under hydrogen flow rates of 30 and 5 mL min^{-1}, respectively. In the graphs, the stages are divided by dash-dot-dash vertical lines. For comparison, the results from the literature[3] measured over Pt extrudates with a bentonite binder were added

Journal of Chemical Technology & Biotechnology published by John Wiley & Sons Ltd on behalf of Society of Chemical Industry.

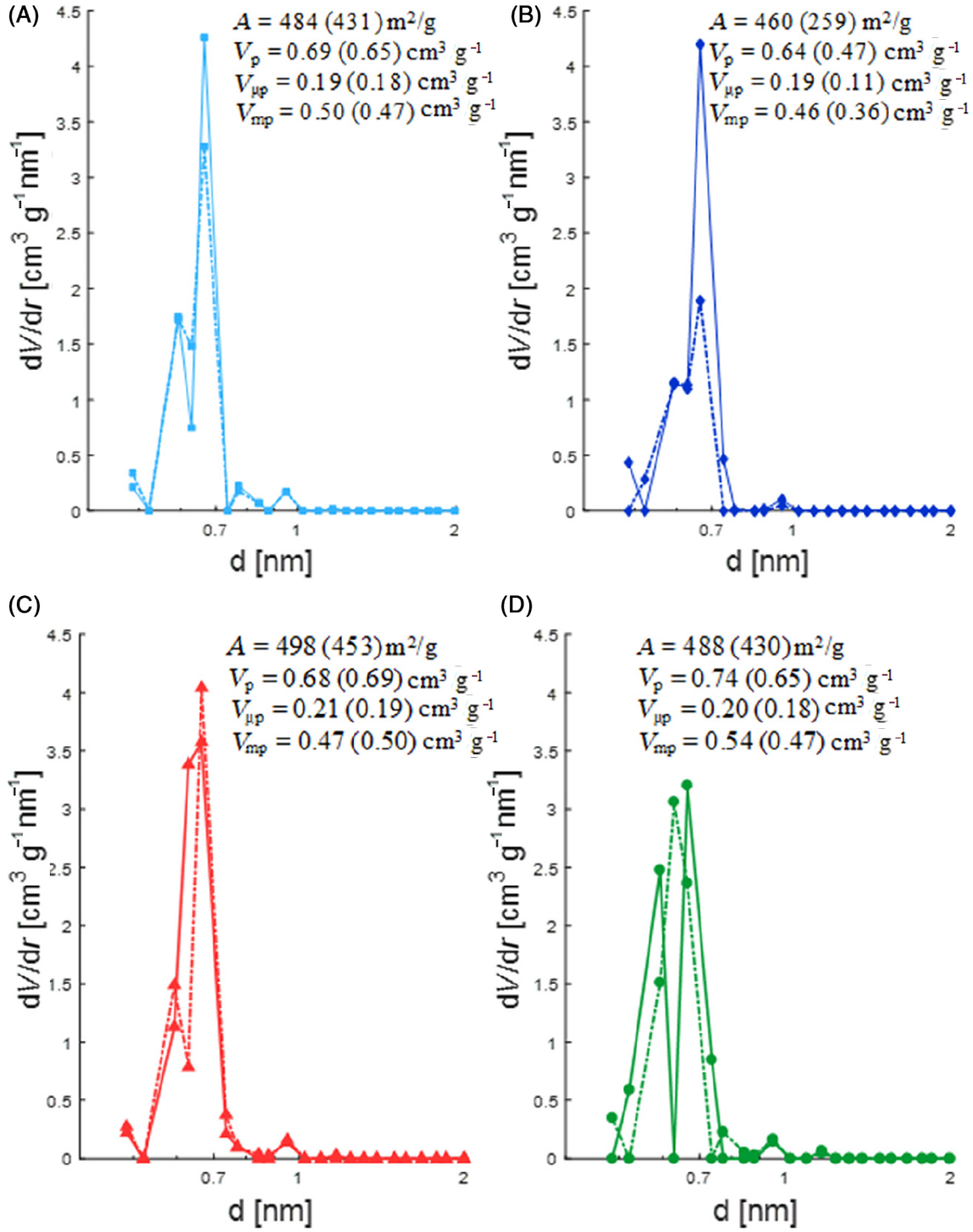

Figure 5. Pore size distribution for fresh (solid line) and spent (dot-dot line, values in parentheses) extrudates: (a) Pt/(H-Beta-25 + Bindzil), post synthesis (light-blue squares); (b) Pt/(H-Beta-25 + Bindzil), *in situ* synthesis (dark-blue diamonds); (c) (Pt/Bindzil) + H-Beta-25 (red triangles); (d) (Pt/H-Beta-25) + Bindzil (green circles). *A*, specific surface area; V_p, specific pore volume; $V_{\mu p}$, micropore volume; V_{mp}, mesopore volume.

to the graphs, showing the results from the first stage of the fresh catalyst obtained in the current work. Catalyst activity and selectivity obtained after 5 min of time-on-stream (TOS) are given in Table 2, together with the best results observed over 3.4% Pt/H-Beta-25 extrudates with bentonite. It should be also mentioned that in this case (denoted by D*) Pt was deposited exclusively on H-Beta-25; the reaction temperature was the same (250 °C), whereas the reaction pressure of 18 bar(a) and hydrogen flow rate of 180 mL min^{-1} were significantly higher, and the reactant contained 1% benzene.[3] For comparison, the data for a slightly higher *n*-hexane conversion obtained over 0.65 wt% Pt/H-Beta powder catalyst and 0.25 wt% Pt/Al_2O_3-Cl industrial extrudates at a similar conversion level (noted as P and I, respectively) were also added to Table 2.[26,44]

Journal of Chemical Technology & Biotechnology published by John Wiley & Sons Ltd on behalf of Society of Chemical Industry.

Table 2. Catalytic results for *n*-hexane hydroisomerization at 5 min time-on-stream

	X (%)	S_{iC6} (%)	S_{DMB} (%)	S_{MP} (%)	S_{ByP} (%)	DMB/MP	2,2-DMB/2,3-DMB	2-MP/3-MP	dX_1/dt (% h^{-1})	dX_2/dt (% h^{-1})	ΔX_{reg} (%)	ΔS_{iC6_reg} (%)	T (°C)	Q_vH_2 (mL min^{-1})	p (bar)	Ref.
A	75	92	25	66	8.2	0.4	1.7	1.6	0.6	2.9	−18	4	250	30	1	CW
B	72	98	20	78	2.0	0.3	1.3	1.6	0.0	0.9	−55	−15	250	30	1	CW
C	31	94	13	81	5.7	0.2	0.4	1.6	4.9	4.5	6	−13	250	30	1	CW
D	74	97	23	75	2.7	0.3	1.6	1.6	0.3	1.9	−23	−3	250	30	1	CW
D*	23	93	8	85	7.4	0.1	0.3	1.6	—	—	—	—	250	180	18	3
P	84	97	34	64	2.8	0.5	2.5	1.5	—	—	—	—	250	22	2.7	26
I	75	99	28	72	1.0	0.4	1.1	1.8	1.3*	—	—	—	150	30	30	43

Conditions: 250 °C, 1 bar, 30 (5) mL min^{-1} H_2, 3 g of catalyst.
A: Pt/(H-Beta-25 + Bindzil), post synthesis; B: Pt/(H-Beta-25 + Bindzil), *in situ* synthesis; C: (Pt/Bindzil) + H-Beta-25; D: (Pt/H-Beta-25) + Bindzil; D*: data from literature[3] for (Pt/H-Beta-25) + bentonite extrudates; *X*: *n*-hexane conversion; P: data from literature[26] for 0.65 wt% Pt/H-Beta powder catalyst; I: data from literature[44] for 0.25 wt% Pt/Al_2O_3-Cl industrial extrudates. *Conversion decline per hour calculated between 2 and 20 TOS; S_{iC6}: selectivity to C_6 isomers (S_{DMB} + S_{MP}); S_{DMB}: selectivity to dimethylbutanes (2,2-DMB + 2,3-DMB); S_{MP}: selectivity to methylpentanes (2-MP, 3-MP); S_{ByP}: selectivity to by-products (mostly cracked C_5-hydrocarbons + C_7 traces); dX_1/dt: conversion decline per hour in the first stage for the fresh catalyst; dX_2/dt: conversion decline per hour in the second stage for the fresh catalyst; ΔX_{reg}: a difference of conversion between the first point over the fresh catalyst and the first point over the regenerated catalyst; ΔS_{iC6_reg}: difference of C_6 isomers selectivity between the first point over the fresh catalyst and the first point over the regenerated catalyst; T: reaction temperature: Q_vH_2: volume flow rate of hydrogen; p: reaction pressure; CW: current work.

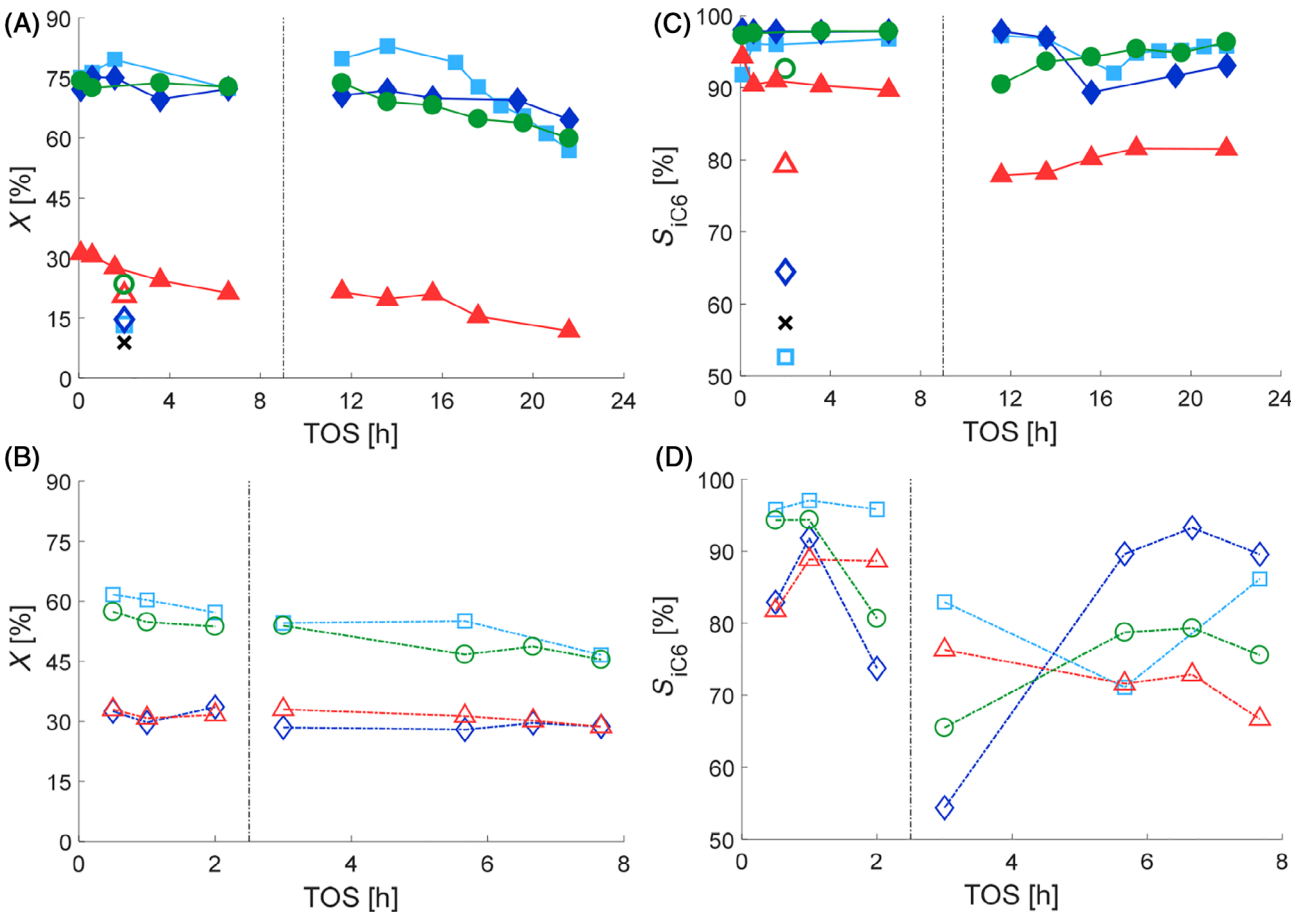

Figure 6. Conversion as a function of TOS: (a) fresh; (b) regenerated extrudates. Selectivity to C_6 isomers as a function of TOS: (c) fresh; (d) regenerated extrudates. Pt/(H-Beta-25 + Bindzil), post synthesis (light-blue squares); Pt/(H-Beta-25 + Bindzil), *in situ* synthesis (dark-blue diamonds); (Pt/Bindzil) + H-Beta-25 (red triangles); (Pt/H-Beta-25) + Bindzil (green circles); literature data:[3] Pt/(H-Beta-25 + bentonite), post synthesis (light-blue squares, open symbols in figure (a, c); Pt/(H-Beta-25 + bentonite), *in situ* synthesis (dark-blue diamonds, open symbols in figure (a, c); (Pt/bentonite) + H-Beta-25 (red triangles, open symbols in figure (a, c); (Pt/H-Beta-25) + bentonite (green circles, open symbols in figure (a, c); pristine H-Beta-25 powder catalyst (black cross).

Journal of Chemical Technology & Biotechnology published by John Wiley & Sons Ltd on behalf of Society of Chemical Industry.

Figure 6(a) illustrates that catalysts A, B and D have high and comparable activity (X = 72–75%, Table 2), with a negligible conversion decline (dX_1/dt = 0–0.6% h^{-1}; Table 2) in the first stage. Comparable results (X = 75%, dX/dt = 1.3% h^{-1}) were obtained over 0.25 wt% Pt/Al_2O_3–7.8 wt% Cl industrial extrudates with the same size as in the current work (1.5 × 3.0 mm) at 150 °C, 30 bar and H_2 flow rate of 30 mL min^{-1}.[44] Conversely, for catalyst C, where Pt is located exclusively on the Bindzil binder, ~ 2.4-fold lower conversion was observed, with a significant activity decline (4.9% h^{-1}). As a comparison, Pt extrudates containing bentonite binder and pristine H-Beta-25 powder exhibited a very low conversion (X = 9–23%;[3] Fig. 6(a)), measured under a higher H_2 flow rate (180 mL min^{-1}) and pressure (18 bar). Conversely, a slightly higher conversion of *n*-hexane (84%, Table 2)[26] was obtained over 0.65% Pt/H-Beta zeolite in a powder form (<150 μm) without a binder at the same temperature of 250 °C, similar H_2 flow rate (22 mL min^{-1}) and pressure (2.7 bar). Although *n*-hexane conversion was close to equilibrium (86.7%), the C_6 isomers per se were not in equilibrium with each other. The major isomerization products were 2-MP, 3-MP and DMB, in that order,[26] similar to observations in the literature for Pt/zeolite catalysts,[3,19,23–25,45] $Al_2O_3/ZrO_2/SO_4/Pt$ catalysts,[28] Pt/Al_2O_3-Cl industrial catalyst[44] and also in the current work.

In the first stage, a high selectivity to the desired C_6 isomers (dimethylbutanes + methylpentanes) reaching 92–98% was obtained over all Pt/H-Beta-25-Bindzil extrudates (Table 2 and Fig. 6(c)). Similar selectivity was observed over the industrial extrudates Pt/Al_2O_3-Cl (<1% of cracked products; I in Table 2),[44] the powder Pt/H-Beta catalyst without a binder (97%; P in Table 2),[26] and Pt/H-Beta-25-bentonite extrudates with the closest proximity between Pt and acid sites (93%; D* in Table 2).[3] Significantly lower selectivity to C_6 isomers (53–79%, literature[3]) was observed over Pt/H-Beta-25-bentonite extrudates, where Pt was deposited on the bentonite binder, or randomly on both zeolite and the binder in the entire shaped body or on the outmost layer of extrudates (Fig. 6(c)). An explanation for lower selectivity to C_6 isomers over Pt/H-Beta-25-bentonite catalyst compared to other extrudates synthesized with Bindzil as a binder can be related to the side products formed because of substantial acidity of the bentonite binder. Furthermore, presence of impurities such as Fe_2O_3, MgO, K_2O in bentonite can also attribute to formation of side products.[30,31]

Figure 7(a, b) displays a correlation of selectivity to C_6 isomers with the metal-to-acid site ratio (c_{Pt}/c_{AS}, Fig. 7(a)) and Pt dispersion (D, Fig. 7(b)). The highest initial C_6 isomer selectivity and at the same time the lowest by-product selectivity were obtained for catalyst B, with the lowest c_{Pt}/c_{AS} ratio and random deposition of Pt in the entire body of extrudates. The second highest initial selectivity to C_6 isomers was obtained for the catalyst D, where Pt was located exclusively on H-Beta-25 zeolite. The main by-products were C_5 isomers and, to a lesser extent, C_1–C_4 hydrocarbons.

The same trend – a decreased selectivity to isomerization with increasing c_{Pt}/c_{AS} ratio – was observed over Pt/R_Si powder catalyst in *n*-heptane hydroisomerization at 350 °C and atmospheric pressure.[4] Conversely, an opposite trend was reported for ethylcyclohexane hydroconversion at 330 °C and 10 bar over $Pt\text{-}Al_2O_3$/HEU-1 pellets (250–500 μm) where Pt was located on the alumina binder.[1] At the maximum ethylcyclohexane conversion of 96%, the selectivity of isomerization, cracking, ring opening and dehydrogenation was 65%, 16%, 2% and 15%, respectively. Different platinum concentrations from 0.1% to 2.3% led to different c_{Pt}/c_{AS} ratios ranging from 0.03 to 0.48. Some sort of a selectivity plateau was reached at a c_{Pt}/c_{AS} ratio of 0.3 for ethylcyclohexane hydroconversion. The isomerization selectivity increased with increasing c_{Pt}/c_{AS} ratio also in the case of Pt/H-Beta-25-bentonite extrudates in *n*-hexane hydroisomerization with the presence of 1% benzene at low temperature (200, 250 °C) and 18 bar, but the plateau was not reached even for a very high c_{Pt}/c_{AS} ratio of 1.12.[3] At the maximum *n*-hexane conversion of 23.4% obtained at 250°C with the extrudates where Pt was located on the zeolite, selectivity of isomerization and cracking was 92.6% and 0.7%, respectively. It should be also mentioned that at high temperature (300–350 °C), selectivity to C_6 isomers was not affected by c_{Pt}/c_{AS} ratio.[3] It can be concluded that the reaction temperature has a larger effect on C_6 isomer selectivity than catalyst acidity.

In the first stage, however, selectivity to C_6 isomers was constant with TOS for all catalysts except catalyst C during 5–35 min of TOS (Fig. 6(c)), for which it was decreasing. A detailed analysis of the results showed that selectivity to dimethylbutanes (DMB, Fig. 8 (a)) decreased, while selectivity to methylpentanes (MP, Fig. 8(c)) increased with TOS. Such behavior can be explained by gradual catalyst deactivation influencing selectivity in the network comprising consecutive reactions from *n*-hexane to methylpentane and further to dimethylbutanes.

Overall selectivity to DMB and MP can be attributed to the presence of strong Brønsted acid sites (sBAS; Table 1 and Fig. 7(c, d)). Figure 7(c, d) shows that selectivity to DMB and MP displays opposite behavior, decreasing and increasing, respectively, with increasing sBAS leading to different DMB/MP ratios of 0.2–0.4 (Table 2). In agreement with the reasoning above, a significantly lower DMB/MP ratio (0.002–0.1), i.e. lower selectivity

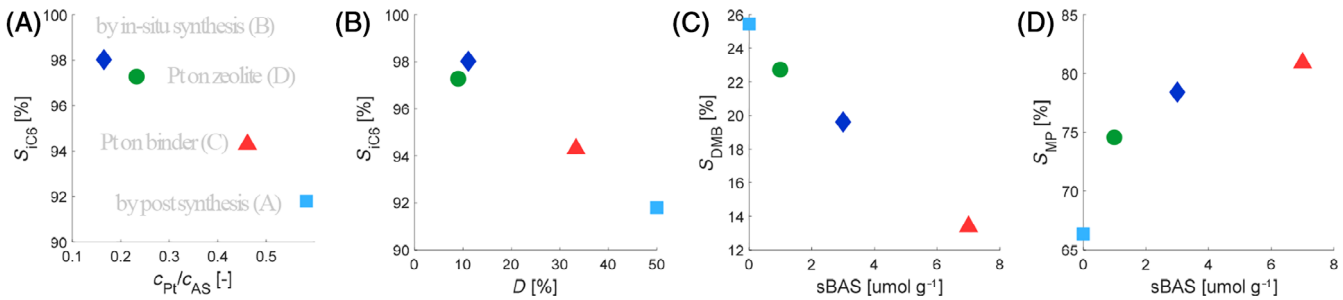

Figure 7. Hydroisomerization of *n*-hexane at 5 min of time-on-stream. Conditions: 250 °C, 1 bar, 30 mL min^{-1} H_2, 3 g catalyst: (a, b) selectivity to C_6 isomers as a function of the metal-to-acid site ratio and of the Pt dispersion; (c) selectivity of dimethylbutanes (DMB); (d) selectivity of methylpentanes (MP) as a function of the strong Brønsted acid sites (sBAS). Pt/(H-Beta-25 + Bindzil), post synthesis (light-blue square); Pt/(H-Beta-25 + Bindzil), *in situ* synthesis (dark-blue diamond); (Pt/Bindzil) + H-Beta-25 (red triangle); (Pt/H-Beta-25) + Bindzil (green circle).

Journal of Chemical Technology & Biotechnology published by John Wiley & Sons Ltd on behalf of Society of Chemical Industry.

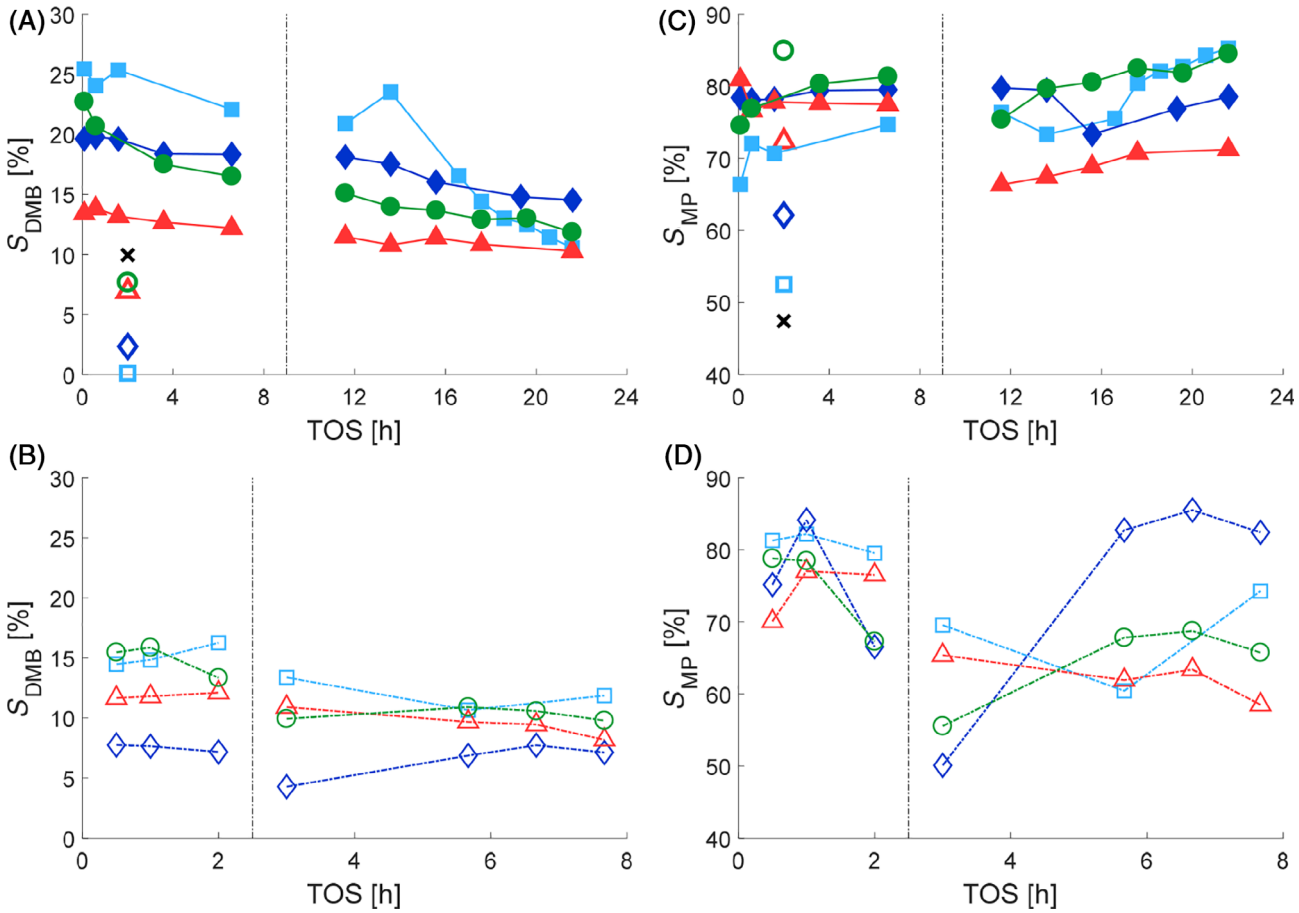

Figure 8. Selectivity to dimethylbutanes as a function of time-on-stream (TOS): (a) fresh; (b) regenerated extrudates. Selectivity to methylpentanes as a function of TOS: (c) fresh; (d) regenerated extrudates. Pt/(H-Beta-25 + Bindzil), post synthesis (light-blue squares); Pt/(H-Beta-25 + Bindzil), *in situ* synthesis (dark-blue diamonds); (Pt/Bindzil) + H-Beta-25 (red triangles); (Pt/H-Beta-25) + Bindzil (green circles); Pt/(H-Beta-25 + bentonite), post synthesis (light-blue squares, open symbols in figure (a, c)); literature data:[3] Pt/(H-Beta-25 + bentonite), *in situ* synthesis (dark-blue diamonds, open symbols in figure (a, c)); (Pt/bentonite) + H-Beta-25 (red triangles, open symbols in figure (a, c)); (Pt/H-Beta-25) + bentonite (green circles, open symbols in figure (a, c)); pristine H-Beta-25 powder catalyst (black cross).

to DMB, was observed for Pt/H-Beta-25-bentonite extrudates with significantly higher amounts of strong Brønsted acid sites (12–129 μmol g^{-1})[3] compared to Pt/H-Beta-25-Bindzil extrudates (sBAS of 0–7 μmol g^{-1}; Table 1).

The negative effect of strong acid sites on the formation of the desired DMB is in line with the literature,[24] where it was shown that strong and the highly dense acid sites can promote hexane cracking. The relative importance of cracking via *β*-scission also increases with increased *n*-hexane conversion.[46] Based on the kinetic model developed in the literature,[46] the only cracking route in hexane hydroconversion is propane formation from 2MP. Taking this and the product distribution of by-products composed mostly of cracked C_5-hydrocarbons into account, it can be assumed that the cracked product is formed predominantly from polymerization–cracking cycles rather than from direct hexane cracking, in line with the literature.[47]

The thermodynamic equilibrium composition at 250 °C is 38.8% 2,2-DMB, 25.0% 2-MP, 12.9% 3-MP, 10.0% 2,3-DMB and 13.3% *n*-hexane.[26] In all cases of Pt/H-Beta-25-Bindzil extrudates, methylpentanes (2-MP/3-MP ratio of 1.6; Table 2) were formed almost at their equilibrium ratio (2-MP/3-MP_{eq} = 1.5).[16] The same results were observed in the literature over the powder Pt-zeolite catalysts (2-MP/3-MP ratio of 1.5–1.7),[16,19,23–26,28,45]) over Pt/H-Beta-25-bentonite extrudates (2-MP/3-MP ratio of 1.4–1.6),[3] and over Pt/Al_2O_3-Cl industrial extrudates (2-MP/3-MP ratio of 1.8)[44] in *n*-hexane hydroisomerization. It is assumed that the reaction rates of protonated cyclopropyl branching of *n*-hexane towards 2-MP and 3-MP are equal. Furthermore, an additional isomerization step is expected from 3MP to 2MP through an alkyl shift with the rate approximately three orders of magnitude larger, which compensates for the identical rates of branching in a previous step.[46] This is in line with an experimentally observed higher selectivity to 2-methylpentane.

Conversely, 2,2-dimethylbutane to 2,3-dimethylbutane ratio (2,2-DMB/2,3-DMB = 0.4–1.7; Table 2) was different for all extrudates and at the same time was significantly lower than the equilibrium value (2,2-DMB/2,3-DMB_{eq} = 2.5).[16] This is attributed to the strong effect of *n*-hexane conversion, as in the case for Pt/Beta powder catalysts,[3,16,19,24–26,44] with both kinetic and thermodynamic factors limiting formation of dimethylbutanes.[47] This result confirms that branching occurs by consecutive reactions, i.e. MP is formed very rapidly and exclusively by isomerization of the protonated cyclopropyl (PCP) at low conversions (<50%). Upon increasing *n*-hexane conversion the yield of DMB increases.[16,24,45,46] Formation of DMB is slower and requires two successive branching steps via protonated cyclopropanes on the

Journal of Chemical Technology & Biotechnology published by John Wiley & Sons Ltd on behalf of Society of Chemical Industry.

acid sites, which are the limiting ones in the bifunctional mechanism. In addition, 2,2-DMB is formed even more slowly than 2,3-DMB.[16] Generation of this 2,2-DMB isomer containing a quaternary carbon atom requires the longest contact time and the strongest acidity.[47] A possible explanation could be the existence of a transformation step from a stable *tert*-2,3-dimethylbutane cation to a sterically hindered and less stable *sec*-2,2-dimethyl-3-butyl cation. Accordingly, the kinetic factors become limiting to achieve equilibrium on all apart from the strongest acid sites due to slow carbocation rearrangements involved in the formation of these quaternary isomers.[16,45,47]

In the second stage of experiments with fresh catalysts (under a lower H_2 flow rate of 5 mL min^{-1}), significant changes in both conversion and selectivity were observed. A 4.8-fold faster catalyst deactivation was observed for catalysts A and D. In the case of catalyst B, the conversion decline increased from 0 to 0.9% per hour. The fastest deactivation and the largest decrease in selectivity to C_6 isomers (i.e. the most prominent increase of by-products; Fig. 7) was observed for catalyst C, where Pt was deposited on the Bindzil binder, i.e. with the second maximal distance between the metal and acid sites (Fig. 1) and the second highest c_{Pt}/c_{AS} ratio (0.54; Table 1). This is contrary to literature reports[5,9,20,48,49] when a decrease in c_{Pt}/c_{AS} ratio promoted faster deactivation; namely, the ratio below 0.03 resulted in rapid deactivation, while very slow or no deactivation was achieved for $c_{Pt}/c_{AS} \geq 0.1$ in the *n*-C_7 and *n*-C_{10} transformations over Pt/H-Y and Pt/H-MOR catalysts. Based on the experimental data obtained in the current work, it can be tentatively concluded that not only the metal-to-acid sites ratio or their proximity influences catalyst deactivation.

A delayed response to changes in the conditions was observed for catalysts A and B with random deposition of Pt on both the zeolite and the binder. This led to a significant decrease in C_6 isomer selectivity at 16 h of TOS. Thereafter, selectivity to C_6 isomers increased with TOS in the same way as was observed for catalysts C and D right from the beginning of the second stage (i.e. from 11.6 h of TOS). Nevertheless, the final selectivity to C_6 isomers (at 21.6 h of TOS) was lower than at the end of the first stage (at 6.6 h of TOS). A significant decrease by 10% and 5% was observed for catalysts C and B, respectively. For catalysts A and D, the final C_6 isomer selectivity was comparable, exhibiting a decrease of only 1%.

Overall, for fresh extrudates, the most stable catalytic activity was obtained with catalyst B, where Pt was distributed uniformly in the entire shaped body randomly on both H-Beta-25 zeolite and on the Bindzil binder (Figs 1 and 8(a)). A very slow deactivation and at the same time a high selectivity to the desired C_6 isomers was obtained with catalyst D, where Pt was deposited exclusively on H-Beta-25 zeolite (Figs 1 and 8(b)). A plausible explanation for slow deactivation Pt/H-Beta-25-Bindzil extrudates where Pt is deposited on the H-Beta-25 zeolite is the coke resistance property of Beta zeolite.[24] Furthermore, changes in the concentration of Brønsted acid sites after introduction of Pt (i.e. low amount of strong BAS compared to the metal-free extrudates; Table 1) can also contribute to coke resistance[26,43,50,51] and enhance formation of the desired C_6 isomers.

Regeneration of the catalyst after ~24 h of TOS had a different effect on different catalysts, depending on Pt location (Table 2 and Figs 6, 8). Only for catalyst C with Pt deposited on the binder was a significant increase in catalytic activity, namely by 64% and 6%, observed compared to the last point before catalyst regeneration and to the first point measured over the fresh catalyst, respectively. Regeneration of the catalyst had a minimal effect on catalysts A and D, illustrated by ~20% lower conversion than for the first point over the fresh catalysts. Unexpectedly, a substantial decrease in the conversion by 50% and 55% was observed for catalyst B compared to the last point before catalyst regeneration and to the first point measured over the fresh catalyst, respectively. On the other hand, in the second stage after regeneration (Fig. 6(b)), conversion over catalyst B was fairly stable. For other catalysts (A, C, D), ~3% h^{-1} of the conversion decline was observed, pointing clearly at catalyst deactivation (Fig. 6(d)). Selectivity to the desired products was lower for all regenerated catalysts. DMB selectivity (Fig. 8(d)) was significantly different with TOS, while MP selectivity (Fig. 8(b)) was almost constant. Comparison of total changes in catalyst activity and selectivity with characterization results of fresh and spent catalyst revealed some correlations, illustrated in Fig. 9.

In line with the literature,[1,5,9,20,26,52] deactivation of the solid acid catalyst is attributed to coke formation. The total decline of *n*-hexane conversion (the first point of the fresh catalyst to the final point of the regenerated catalyst) was correlated with changes in the textural properties of the deactivated catalysts (Fig. 9(a, b)). The total decrease in selectivity to C_6 isomers

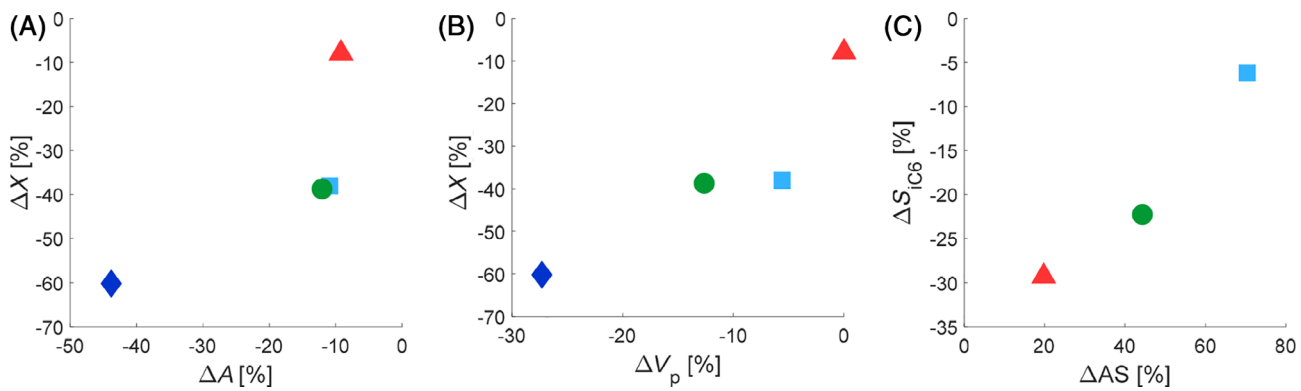

Figure 9. Difference of *n*-hexane conversion (between the last point of the regenerated catalyst and the first point of the fresh catalyst) as a function of: (a) difference in the specific surface area; (b) difference in the pore volume (between spent and fresh catalyst); and (c) difference of C_6 isomer selectivity (between the last point of the regenerated catalyst and the first point of the fresh catalyst) as a function of the difference of total acid sites (between spent and fresh catalyst). Pt/(H-Beta-25 + Bindzil), post synthesis (light-blue square); Pt/(H-Beta-25 + Bindzil), *in situ* synthesis (dark-blue diamond); (Pt/Bindzil) + H-Beta-25 (red triangle); (Pt/H-Beta-25) + Bindzil (green circle).

Journal of Chemical Technology & Biotechnology published by John Wiley & Sons Ltd on behalf of Society of Chemical Industry.

increased with increasing acid sites of the deactivated catalyst (Fig. 9(c)). Apparently, no correlations between the sintering of metal particles and the different behavior of catalysts during the deactivation process could be seen.

A direct comparison with the published data is very difficult due to utilization of different types of catalysts (e.g. supports, metals and their loading), different reaction conditions and reactors. However, overall, it can be stated that in the current work, by using Pt/H-Beta-25 extrudates with Bindzil as a binder similar or better catalytic activity (X = 74%; Table 2D) and selectivity to C_6 isomers (S_{iC6} = 97%; Table 2D) at 250 °C were obtained than in the literature for Pt bifunctional catalysts at 240–280 °C (X ~ 5–82, S_{iC6} ~ 40–99%).[16,19,23–26,46,47,53,54]

In general, Beta-based catalysts are considered relatively catalytically stable in *n*-hexane hydroisomerization,[24,26,54] especially compared to mordenite-based catalysts, giving a conversion decline of respectively 6%[16] and 35% h^{-1}.[24] Such significant catalyst deactivation was explained by the higher acid site density and the unidimensional pore system of mordenite catalysts.[24] Only slight changes in the catalytic activity of *n*-hexane and selectivity to C_6 isomers were observed over Pt/Beta catalysts up to ~12 h (0.3% h^{-1}),[26] 13 h[54] and 55 h (0.03% h^{-1}).[24] This is in line with the results over Pt extrudates B (0% h^{-1}; Table 2) and D (0.3% h^{-1}; Table 2) tested in the first stage (up to 7 h) in the current work.

Considering that the selectivity of the individual mono- and di-branched products are strongly influenced by *n*-hexane conversion[19,24–26,47] and by the catalyst type,[24] these results were compared only with the literature data obtained over Pt/Beta catalysts at a similar conversion level and reaction temperature to those in the current work.

The distribution of the desired products and selectivity to methylpentanes (S_{MP} = 75%; Table 2) and dimethylbutanes (S_{DMB} = 23%; Table 2) were significantly better for D shaped catalyst than for 0.6% Pt/Beta catalyst (S_{MP} = 35%, S_{DMB} = 7%, catalyst fraction = 1.2–2.4 mm, X = 72%, 250 °C)[54] and the same (except for the 2,2-DMB/2,3-DMB ratio) as for 0.5% Pt/H-Beta catalyst at a higher temperature (S_{MP} = 76%, S_{DMB} = 23%, 2,2-DMB/2,3-DMB = 0.8, 2-MP/3-MP = 1.6, X = 73%, 275 °C).[24]

CONCLUSIONS

This work describes the preparation of bifunctional catalysts in the form of extrudates with controlled metal (platinum) deposition on either a zeolite H-Beta-25, a silica (Bindzil) binder or randomly on both. In the last cases shaping was done either prior to or before deposition of platinum, resulting in the metal location mostly in the outer layer of extrudates or randomly in the entire volume, respectively. All four catalysts contained the same Pt nominal loading, i.e. 2 wt%, and 70/30 weight ratio of H-Beta-25 zeolite/Bindzil binder. Catalytic behavior and regeneration were investigated using *n*-hexane hydroisomerization as a model reaction in a fixed-bed reactor. The catalytic tests were performed at 250 °C, atmospheric pressure and hydrogen flow rate of 5 or 30 mL min^{-1}. After the reaction, the catalysts were regenerated using calcination at 600 °C for 3 h, subsequent flushing with nitrogen and reduction under hydrogen at 400 °C for 1 h before reuse.

TEM images confirmed that location of the metal (Pt) in the extrudates can be successfully regulated using the preparation strategy adopted in the current work. Extrudates with different mechanical strength, Pt particle size, number of acid sites (Brønsted and Lewis) and their strength, the metal-to-acid site (c_{Pt}/c_{AS}) ratio and proximity between these two types of active sites were obtained, while the textural properties were comparable.

The catalysts exhibited high selectivity to C_6 isomers, with the major isomerization products being 2-methylpentane, 3-methylpentane and dimethylbutane, in that order. Selectivity to C_6 isomers was correlated with the metal-to-acid site ratio and Pt dispersion. The ratio of dimethylbutanes to methylpentanes and 2,2-dimethylbutane to 2,3-dimethylbutane was increased with decreasing strong Brønsted acid sites of catalysts and increasing *n*-hexane conversion. At the same time, the ratio of 2-methylpentane to 3-methylpentane ratio was the same for all extrudates.

A significantly faster deactivation and more prominent decrease of selectivity to C_6 isomers was observed for the catalyst where Pt was deposited on the Bindzil binder, i.e. with the second maximal distance between the metal and acid sites and the second highest c_{Pt}/c_{AS} ratio. This led to the conclusion that the location of the metal can have a larger influence on catalyst deactivation rather than metal-to-acid site ratio or their proximity. Only for this catalyst was the regeneration of spent catalyst successful. Conversely, a very slow deactivation and at the same time high selectivity to the desired C_6 isomers was obtained for the catalyst where Pt was deposited solely on H-Beta-25 zeolite, i.e. with the minimal distance between the metal to acid sites, the second lowest c_{Pt}/c_{AS} ratio, and absence of strong Brønsted acid sites.

ACKNOWLEDGEMENTS

The authors are grateful to the Academy of Finland for funding through the project 'Synthesis of spatially controlled catalysts with superior performance'.

REFERENCES

1 Gutierrez-Acebo E, Leroux C, Chizallet C, Schuurman Y and Bouchy C, Metal/acid bifunctional catalysis and intimacy criterion for ethylcyclohexane hydroconversion: when proximity does not matter. *ACS Catal* **8**:6035–6046 (2018).
2 Mendes PSF, Silva JM, Ribeiro MF, Daudin A and Bouchy C, From powder to extrudate zeolite-based bifunctional hydroisomerization catalysts: on preserving zeolite integrity and optimizing Pt location. *J Ind Eng Chem* **62**:72–83 (2018).
3 Vajglová Z, Kumar N, Peurla M, Hupa L, Semikin K, Sladkovskiy DA *et al.*, Effect of the preparation of Pt-modified zeolite Beta-Bentonite extrudates on their catalytic behavior in *n*-hexane hydroisomerization. *Ind Eng Chem Res* **58**:10875–10885 (2019).
4 Samad JE, Blanchard J, Sayag C, Louis C and Regalbuto JR, The controlled synthesis of metal–acid bifunctional catalysts: the effect of metal:acid ratio and metal–acid proximity in Pt silica–alumina catalysts for *n*-heptane isomerization. *J Catal* **342**:203–212 (2016).
5 Batalha N, Pinard L, Pouilloux Y and Guisnet M, Bifunctional hydrogenating/acid catalysis: quantification of the intimacy criterion. *Catal Lett* **143**:587–591 (2013).
6 Sahu R, Song BJ, Im JS, Jeon YP and Lee CW, A review of recent advances in catalytic hydrocracking of heavy residues. *J Ind Eng Chem* **27**:12–24 (2015).
7 Primo A and Garcia H, Zeolites as catalysts in oil refining. *Chem Soc Rev* **43**:7548–7561 (2014).
8 Weitkamp J, Catalytic hydrocracking: mechanisms and versatility of the process. *ChemCatChem* **4**:292–306 (2012).
9 Alvarez F, Ribeiro FR, Perot G, Thomazeau C and Guisnet M, Hydroisomerization and hydrocracking of alkanes: influence of the balance between acid and hydrogenating functions on the transformation of *n*-decane on PtHY catalysts. *J Catal* **162**:179–189 (1996).
10 Harmel J, van der Wal LI, Zecevic J, de Jongh PE and de Jong KP, Influence of intimacy for metal–mesoporous solid acids catalysts for *n*-alkanes hydro-conversion. *Cat Sci Technol* **10**:2111–2119 (2010).

11 Chica A and Corma A, Hydroisomerization of pentane, hexane, and heptane for improving the octane number of gasoline. *J Catal* **187**: 167–176 (1999).
12 Stojkovic N, Vasic M, Marinkovic M, Randjelovic M, Purenovic M, Putanov P *et al*., A comparative study of *n*-hexane isomerization over solid acids catalysts: sulfated and phosphated zirconia. *Chem Ind Chem Eng Q* **18**:209–220 (2012).
13 Weber JL, Krans NA, Hofmann JP, Hensen EJM, Zecevic J, de Jongh PE *et al*., Effect of proximity and support material on deactivation of bifunctional catalysts for the conversion of synthesis gas to olefins and aromatics. *Catal Today* **342**:161–166 (2020).
14 Samad JE, Blanchard J, Sayag C, Louis C and Regalbuto JR, The controlled synthesis of metal–acid bifunctional catalysts: selective Pt deposition and nanoparticle synthesis on amorphous aluminosilicates. *J Catal* **342**:213–225 (2016).
15 Murzin DY, Mesolevel bifunctional catalysis. *Kinet Catal* **61**:80–92 (2020).
16 Sousa BV, Brito KD, Alves JJN, Rodrigues MGF, Yoshioka CMN and Cardoso D, *n*-Hexane isomerization on Pt/HMOR: effect of platinum content. *React Kinet Mech Catal* **102**:473–485 (2011).
17 Zecevic J, Vanbutsele G, de Jong KP and Martens JA, Nanoscale intimacy in bifunctional catalysts for selective conversion of hydrocarbons. *Nature* **528**:245–248 (2015).
18 Akhmedov VM and Al-Khowaiter SH, Recent advances and future aspects in the selective isomerization of high *n*-alkanes. *Catal Rev Sci Eng* **49**:33–139 (2007).
19 van de Runstraat A, Kamp JA, Stobbelaar PJ, van Grondelle J, Krijnen S and van Santen RA, Kinetics of hydro-isomerization of *n*-hexane over platinum containing zeolites. *J Catal* **171**:77–84 (1997).
20 Guisnet M, 'Ideal' bifunctional catalysis over Pt–acid zeolites. *Catal Today* **218**:123–134 (2013).
21 de Lucas A, Sanchez P, Funez A, Ramos MJ and Valverde JL, Liquid-phase Hydroisomerization of *n*-octane over platinum-containing zeolite-based catalysts with and without binder. *Ind Eng Chem Res* **45**:8852–8859 (2006).
22 Dorado F, Romero R and Canizares P, Hydroisomerization of *n*-butane over Pd/HZSM-5 and Pd/H Beta with and without binder. *Appl Catal A* **236**:235–243 (2002).
23 Lee JK, Lee HT and Rhee HK, Isomerization of *n*-hexane over platinum loaded zeolites. *React Kinet Catal Lett.* **57**:323–337 (1996).
24 Yashima T, Wang ZB, Kamo A, Yoneda T and Komatsu T, Isomerization of *n*-hexane over platinum loaded zeolite catalysts. *Catal Today* **29**: 279–283 (1996).
25 Hollo A and Hancsok J, Skeletal isomerization of *n*-hexane over platinum-loaded H-Mordenite. *J Ind Chem* **25**:153–155 (1997).
26 Chu HY, Rosynek RP and Lunsford JH, Skeletal isomerization of hexane over Pt/H-Beta zeolites: is the classical mechanism correct? *J Catal* **178**:352–362 (1998).
27 Chen IY, Chu MC, Liaw JS and Wang CC, Two-phase flow characteristics across sudden contraction in small rectangular channels. *Exp Therm Fluid Sci* **32**:1609–1619 (2008).
28 Chuparev EV, Zernov PA, Parputs OI and Lisitsyn NV, Low temperature isomerization of *n*-hexane on catalyst systems $Al_2O_3/ZrO_2/SO_4$/Pt. *Russ J Appl Chem* **87**:767–772 (2014).
29 Azkaar M, Mäki-Arvela P, Vajglová Z, Fedorov V, Kumar N, Hupa L *et al*., Synthesis of menthol from citronellal over supported Ru- and Pt-catalysts in continuous flow. *React Chem Eng* **4**:2156–2169 (2019).
30 Vajglová Z, Kumar N, Peurla M, Peltonen J, Heinmaa I and Murzin DY, Synthesis and physicochemical characterization of Beta zeolite–Bentonite composite materials for shaped catalysts. *Catal Sci Technol* **8**:6150–6162 (2018).
31 Vajglová Z, Kumar N, Mäki-Arvela P, Eränen K, Peurla M, Hupa L *et al*., Effect of binders on the physicochemical and catalytic properties of extrudate-shaped Beta zeolite catalysts for cyclization of citronellal. *Org Process Res Dev* **23**:2456–2463 (2019).
32 Vajglová Z, Kumar N, Mäki-Arvela P, Eränen K, Peurla M, Hupa L *et al*., Synthesis and physicochemical characterization of shaped catalysts of Beta and Y zeolites for cyclization of citronellal. *Ind Eng Chem Res* **58**:18084–18096 (2019).
33 Whiting GT, Meirer F, Mertens MM, Bons AJ, Weiss BM, Stevens PA *et al*., Binder effects in SiO_2- and Al_2O_3-bound zeolite ZSM-5-based extrudates as studied by microspectroscopy. *ChemCatChem* **7**:1312–1321 (2015).
34 Jasra RV, Tyagi B, Badheka YM, Choudary VN and Bhat TSG, Effect of clay binder on sorption and catalytic properties of zeolite pellets. *Ind Eng Chem Res* **42**:3263–3272 (2003).
35 Dorado F, Romero R and Canizares P, Influence of clay binders on the performance of Pd/HZSM-5 catalysts for the Hydroisomerization of *n*-butane. *Ind Eng Chem Res* **40**:3428–3434 (2001).
36 Liu H, Zhou YM, Zhang YW, Bai LY and Tang MH, Influence of binder on the catalytic performance of PtSnNa/ZSM-5 catalyst for propane dehydrogenation. *Ind Eng Chem Res* **47**:8142–8147 (2008).
37 Yue MB, Yang N and Wang YM, Synthesis of shaped ZSM-5 zeolites by dry-gel conversion with seed gel as directing agent. *Acta Phys Chim Sin* **28**:2115–2121 (2012).
38 Song Y, Zhang LL, Li GD, Shang YS, Zhao XM, Ma T *et al*., ZSM-5 Extrudates modified with phosphorus as a super effective MTP catalyst: impact of the acidity on binder. *Fuel Process Technol* **168**:105–115 (2017).
39 Wu X, Alkhawaldeh A and Anthony RG, Investigation on acidity of zeolites bound with silica and alumina. *Stud Surf Sci Catal* **143**:217–225 (2002).
40 Geng CH, Zhang F, Gao ZX, Zhao LF and Zhou JL, Hydroisomerization of *n*-tetradecane over Pt/SAPO-11 catalyst. *Catal Today* **93-95**: 485–491 (2004).
41 Ramos MJ, Gomez JP, Dorado F, Sanchez P and Valverde JL, Hydroisomerization of a refinery naphtha stream over platinum zeolite-based catalysts. *Chem Eng J* **126**:13–21 (2007).
42 Chi KB, Zhao Z, Tian ZJ, Hu S, Yan LJ, Li TS *et al*., Hydroisomerization performance of platinum supported on ZSM-22/ZSM-23 intergrowth zeolite catalyst. *Pet Sci* **10**:242–250 (2013).
43 Kubička D, Kumar N, Venalainen T, Karhu H, Kubickova I, Osterholm H *et al*., Metal–support interactions in zeolite-supported noble metals: influence of metal crystallites on the support acidity. *J Phys Chem B* **110**:4937–4946 (2006).
44 Ducourty B, Szabo G, Dath JP, Gilson JP, Goupil JM and Cornet D, Pt/Al_2O_3-Cl catalysts derived from ethylaluminumdichloride activity and stability in hydroisomerization of C-6 alkanes. *Appl Catal A* **269**: 203–214 (2004).
45 Allain JF, Magnoux P, Schulz P and Guisnet M, Hydroisomerization of *n*-hexane over platinum Mazzite and platinum Mordenite catalysts: kinetics and mechanism. *Appl Catal A* **152**:221–235 (1997).
46 Toch K, Thybaut JW and Marin GB, A systematic methodology for kinetic modeling of chemical reactions applied to *n*-hexane hydroisomerization. *AIChE J* **61**:880–892 (2015).
47 Hattori H, Misono M and Ono Y, *Acid–Base Catalysis II*. Elsevier, Amsterdam (1994).
48 Guisnet M, Alvarez F, Giannetto G and Perot G, Hydroisomerization and hydrocracking of *n*-heptane on PtH zeolites: effect of the porosity and of the distribution of metallic and acid sites. *Catal Today* **1**: 415–433 (1987).
49 Alvarez F, Giannetto G, Guisnet M and Perot G, Hydroisomerization and hydrocracking of *n*-heptane transformation on a Pt-dealuminated Y-zeolite: comparison with a Pt-Y-zeolite. *Appl Catal* **34**:353–365 (1987).
50 Dong XF, Song YB and Lin WM, A new way to enhance the coke-resistance of Mo/HZSM-5 catalyst for methane dehydroaromatization. *Catal Commun* **8**:539–542 (2007).
51 Huang J, Jiang YJ, Marthala VRR, Bressel A, Frey J and Hunger M, Effect of pore size and acidity on the coke formation during ethylbenzene conversion on zeolite catalysts. *J Catal* **263**:277–283 (2009).
52 Guisnet M and Magnoux P, Coking and deactivation of zeolites: influence of the pore structure. *Appl Catal* **54**:1–27 (1989).
53 Cejka J, Zilkova N, Petr N, Molecular sieves: from basic research to industrial applications, in *Proceedings of the 3rd International Zeolite Symposium (3rd FEZA)*, Part 2, Prague, Czech Republic. Elsevier, Amsterdam, pp. 23–26 (2005).
54 Phatanasri S, Praserthdam P, Kularbkeaw S and Panichsarn S, Isomerization of *n*-hexane over platinum ion-exchanged zeolite Beta. *React Kinet Catal Lett* **71**:281–287 (2000).

Journal of Chemical Technology & Biotechnology published by John Wiley & Sons Ltd on behalf of Society of Chemical Industry.